Bull. Chem. Soc. Jpn., 72, 1647—1664 (1999)

Accounts

Photophysical and Photochemical Primary Processes of Diphenylacetylene Derivatives and Related Compounds in Liquid Phase

Yoshinori Hirata

Department of Chemistry, Graduate School of Engineering Science, Osaka University,
1-3 Machikaneyama-machi, Toyonaka 560-8531

(Received March 1, 1999)

Photophysical and photochemical primary processes of diphenylacetylene (DPA) derivatives and related compounds have been reviewed. Curious photophysical properties of the low lying excited singlet states of DPA, such as an exceptionally slow $S_2 \rightarrow S_1$ internal conversion, a distinct temperature effect of the S_2 lifetime, and a strong excitation energy dependence of the fluorescence yield, were correlated with the S_2–S_1 energy gap. Contradictions of the assignments of the lowest excited singlet states of DPA were resolved and the mechanism of the $S_2 \rightarrow S_1$ internal conversion was proposed from the comparison of the dynamic behavior of DPA with that of diphenylpolyenes. The small S_2–S_1 energy gap as well as the large displacement between the potential curves of the upper and lower electronic states can be a reason why the S_2 state of the DPA derivatives is exceptionally long-lived. The DPA derivatives of which the intramolecular charge-separated states are formed in polar solvents were used as probe molecules of the solvent–solute interaction. Significant enhancement of the charge recombination of aminophenyl(phenyl)acetylene in protic solvents should be due to the interaction between amino nitrogen atom of the solute molecule and the hydrogen-bonded solvent oligomer.

A great deal of activities in both experimental and theoretical areas have been devoted to elucidate the mechanism of the radiationless processes such as internal conversion and intersystem crossing.[1,2] By 1968, it was shown that the radiationless transition is essentially the intramolecular process which takes place in the isolated molecule.[3,4] Since the radiationless process competes with the radiative processes such as fluorescence and phosphorescence, we can obtain a lot of information on the radiationless process from the measurements of emission properties. Transient absorption measurements are also useful for the investigation of a system which does not emit fluorescence.

We know the energy gap law, which shows the relation of the transition probability and the energy gap between the origins of the upper and lower electronic states. The rule essentially comes from the Franck–Condon factor of the radiationless transition. Engleman and Jortner derived the transition probability of the radiationless process in the weak coupling limit to be[5]

$$W = \frac{C^2\sqrt{2\pi}}{\hbar\sqrt{2\pi\hbar\omega_M \Delta E}} \exp\left(-\frac{\gamma \Delta E}{\hbar\omega_M}\right), \quad (1)$$

where C^2 is the electronic coupling term, ΔE and ω_M stand for the energy gap and the frequency of the effective accepting mode, and γ is a constant that contains the information about the displacement of the potential energy surfaces in the two electronic states. The transition probability is predicted to be temperature independent and Eq. 1 exhibits roughly exponential dependence on the energy gap, which is experimentally observed in several cases.[6,7] Usually, the S_1–S_0 gaps of aromatic molecules are so large that the $S_1 \rightarrow S_0$ internal conversion cannot compete with the fluorescence and the $S_1 \rightarrow T_1(T_2)$ intersystem crossing. On the other hand, except for a few cases, the energy gaps between the excited singlet states are small and, until recently, the internal conversion to the S_1 state was too fast to observe.

Many of the electron transfer and the chemical reactions are not in the weak coupling limit, but they belong to the strong coupling limit. The transition probabilities in the strong coupling limit are calculated as

$$W = \frac{C^2\sqrt{4\pi}}{\sqrt{E_M \hbar < \omega >}} \exp\left(-\frac{2E_A}{\hbar < \omega >}\right) \quad (2)$$

and

$$W = \frac{k_B T}{\hbar} \frac{C^2\sqrt{2\pi}}{\sqrt{E_M (k_B T)^3}} \exp\left(-\frac{E_A}{k_B T}\right) \quad (3)$$

at low and high temperatures, respectively, where E_M is the reorganization energy, E_A is the energy of the crossing point of potential curves measured from the origin of the upper electronic state, and $< \omega >$ is the mean vibrational frequency. Equation 3 predicts that the transition has the acti-

vation energy of E_A.

Recent developments of the ultrafast laser technology and spectroscopy allow us to observe the dynamic behavior of the higher excited singlet states. In the most cases, the lifetimes of the second excited singlet states fall in the subpicosecond region and their fluorescence is quite weak. There are a few exceptions which fluoresce from higher excited singlet states; most of them have large S_2–S_1 energy gaps. Azulene is known to be the first exception of Kasha's rule: *The emitting level of a given multiplicity is the lowest excited level of that multiplicity.*[8] Many researchers tried to correlate the yield of the anomalous fluorescence of azulene with the size of the energy gap.[9—11] The S_2–S_1 energy gap of azulene is as large as 13400 cm^{-1}. Xanthione also has a large energy gap of about 8000 cm^{-1} and shows the fluorescence from S_2.[12—14]

On the other hand, the interstate coupling between close-lying excited singlet states in the condensed phases was studied for polyenes, dimethylbenzaldehydes, and azuleno[5,6,7-*c*,*d*]phenalene. Azulenophenalene, of which the S_3–S_2 energy gap is about 1050 cm^{-1}, shows a strong $S_3 \rightarrow S_0$ fluorescence in rigid toluene glass at 100 K.[15] Such exceptionally large fluorescence yield was thought to be the results of not only the slow $S_3 \rightarrow S_1$ internal conversion, which is ensured by a large S_3–S_1 energy gap of 8940 cm^{-1}, but of the slow $S_3 \rightarrow S_2$ internal conversion. Because of the small S_3–S_2 energy gap, it was considered that only few vibronic levels in the S_2 manifold is isoenergetic to the vibrationless level of the S_3 state and thus, at low temperatures, the molecules in the S_3 state cannot undergo efficient internal conversion to the S_2 state. This may be the first case which demonstrated the slow internal conversion between the close lying excited singlet states.

Besides the *cis–trans* isomerization, one of the most interesting points of the spectroscopic and photophysical properties of linear polyenes is the ordering of the lowest excited singlet states.[16—18] The first experimental confirmation of a low-lying forbidden S_1 ($2A_g$) state below the one-photon allowed S_2 (B_u) state of *all trans*-1,8-diphenyl-1,3,5,7-octatetraene was given by Hudson and Kohler.[16,17] After that a great deal of efforts have established that the lowest excited singlet state of *all trans*-diphenylpolyenes with a chain length of three double bonds or longer is the A_g state.[19,20] Under the free jet conditions, the 2^1A_g state of 1,4-diphenyl-1,3-butadiene is found to be about 1150 cm^{-1} below the 1^1B_u (S_2) state, which is one-photon allowed from the ground state.[21—23] Environmental effects of the level ordering were also observed. In the liquid phase, inversion of the level ordering of the 2^1A_g and 1^1B_u states due to the solvent assisted conformational stabilization of 1,4-diphenyl-1,3-butadiene was suggested.[24,25] Some diphenylpolyenes are known to emit fluorescence from both the S_1 and S_2 states,[26] but the S_2 fluorescence of diphenylpolyenes with a short chain length is much weaker than that of the S_1 fluorescence. Recently, dynamic behavior of the S_2 state of diphenylpolyenes was investigated by measuring femtosecond transient absorption spectra.[27]

Since DPA and diphenylpolyenes have some similarity in the electronic structure, we are interested in the level ordering of the lowest excited singlet states of DPA derivatives. Environmental effects of the electronic structure and the dynamic behavior were also investigated. There is no doubt that a presence of the C≡C triple bond and a π-conjugation throughout the molecule distinguish the DPA derivatives from the other aromatic molecules. Push–pull type diphenylpolyene derivatives are known to form the charge separated (CS) states in polar solvents and twisting of the phenyl ring is considered to be the important mechanism to break π-conjugation and to stabilize the CS state.[28] Twisting of phenyl rings of DPA derivatives cannot break the π-conjugation but the formation of the intramolecular CS state with a quite large dipole moment was reported for DACN–DPA and MTCN–DPA.[29,30] It should be interesting to study the stabilization mechanism and the structure of the CS state.

Due to the rigid rod-like structure of the DPA derivatives, they can be good probe molecules of the solvation process. To elucidate the solvent–solute interaction, measurements of the rotational relaxation of DACN–DPA were carried out in various solvents.[31] Since directions of the transition dipoles of the first absorption band, the fluorescence band, and the strong transient absorption in the visible region coincide with the molecular long axis, we can analyze the anisotropy decay in a simple manner. Although a large amplitude torsional motion of the phenyl rings is possible, less flexibility compared with diphenylpolyenes may play an important role in the dynamic behavior of excited states.

A complicated electronic structure of DPAs should be due to the presence of two π-orbitals, π_x and π_y, which are perpendicular to each other. DPA in a single crystal is known to take a planar structure of a D_{2h} symmetry in the ground state.[32,33] Therefore we can expect that one π-orbital (π_x) of the acetylene bond is strongly conjugated with the π-orbitals of the phenyl rings. The other π-orbital (π_y) may be localized on the acetylene bond. A much faster intersystem crossing from the excited singlet states to the T_1 state of DPA than those of diphenylpolyenes suggests a quite large enhancement of the spin-orbit coupling due to the excited state with a $\pi_x\pi_y^*$ configuration. The T_1 formation of diphenylpolyenes seems to be negligible and the lifetime of the S_1 state was essentially determined by the $S_1 \rightarrow S_0$ internal conversion and the radiative process. The $S_1 \rightarrow T_1$ intersystem crossing of diphenylbutadiyne (DPB) is almost one order of magnitude faster than that of DPA, which may be due to the decrease of the energy gap between the excited states with $\pi_x\pi_y^*$ and $\pi_x\pi_x^*$ configurations in DPB. An increasing flexibility with increasing carbon chain length may also play an important role in the enhancement of the spin–orbit coupling.

Molecular structures of the triplet state and the radical ions of DPA were investigated by measuring resonance Raman spectra and by using ab initio MO calculations.[34,35] The normal mode analysis was also carried out for these states. On the other hand, a little is known for the excited singlet states. Several vibrational modes in the excited singlet states are known from the CARS measurements,[36,37] but it is difficult to carry out the normal mode analysis of the excited singlet

states in a reliable manner. Acetylene is known to take a bent structure in the excited state and a similar possibility was proposed for DPA in the literature.[36,37] Because of the π-conjugation between the acetylene bond and the phenyl rings of DPA, the excited state may take different structure from the bent form.

The fluorescence state of diphenylacetylene (DPA) is the S_2 state in solution phase. The dynamic behavior of the low-lying excited singlet states seems to be quite different from that of usual aromatic molecules.[38,39] The characters and the energetic ordering of the low lying excited singlet state of DPA are revealed from the one- and two-photon spectroscopy in the supersonic jet[40] and low temperature matrices.[41] In the gas phase, three excited singlet states are located in the first absorption band region.[40] Only one excited singlet state is observed by the steady state measurements in the condensed media,[41] while in addition to the fluorescence state, a dark excited singlet state is observed by the picosecond time resolved measurements.[38,39]

Assignments of the lowest excited singlet states of DPA are not yet established. In order to resolve the contradictions of the assignments of the lowest excited singlet states,[40–42] it is necessary to accumulate more knowledge about the photophysical properties of DPA derivatives and the related compounds. Comparison of the dynamic behavior of the DPA derivatives and diphenylpolyenes can be helpful to shed light on the mechanism of the relaxation process. Figure 1 shows the DPA derivatives that we are going to discuss in this review.

1 Properties of the Low-Lying Excited Singlet States of DPA and DPB

The absorption and fluorescence spectra of DPA and DPB in cyclohexane are displayed in Fig. 2. Both DPA and DPB show a long progression of C≡C stretching modes (ca. 2150 cm^{-1}), which is an indication of the large displacement of the C≡C bond length upon the electronic excitation. In the ground state, the frequency of the C≡C stretching mode is 2220 cm^{-1}.[43] The peaks which can be ascribed to the ring breathing mode (ca. 1000 cm^{-1}) are also observed in both absorption and fluorescence spectra. The breathing mode is weaker in DPB. A mirror symmetric relation between the absorption and fluorescence spectra of DPA is observed, while the fluorescence of DPB is so weak that we cannot distinguish it from the stray light or the Raman scattering of the solvent.[44] The fluorescence quantum yield of DPA was estimated to be about 0.01 in hexane at room temperature, while that of DPB was less than 1×10^{-4}. Integrating the absorption spectra between 33000 and 41500 cm^{-1} for DPA and between 29000 and 36000 cm^{-1} for DPB, the oscillator strengths of the first absorption band of these molecules were calculated to be 0.83 and 0.93 for DPA and DPB, respectively. The radiative lifetimes calculated from the Strickler–Berg relation,[45]

$$1/\tau_r = 2.88\times10^{-9}n^2 < \nu_f^{-3} >_{Av}^{-1} \int \frac{\epsilon d\bar{\nu}}{\bar{\nu}},$$

were about 1.3 and 1.0 ns for DPA and DPB, respectively. In this calculation the same Stokes' shift was assumed for DPA and DPB.

Tanizaki et al. measured dichroic spectra of DPA in stretched poly(vinyl alcohol) sheets and compared the spectra with the results of semi-empirical SCF-CI calculations.[46] The 0–0 transition of the first absorption band appears at 298 nm, while the second absorption band is around 220 nm. The transition moments of the first and the second absorption bands are polarized along the long and short axes, respectively. Their calculations predict that there will be three excited singlet states in the first absorption band region. They are the 1^1B_{1u}, 1^1B_{2u}, and 2^1A_g states. Only the 1^1B_{1u} state has a large oscillator strength from the ground electronic state. The $1^1B_{2u}\leftarrow1^1A_g$ transition is orbitally forbidden, while the $2^1A_g\leftarrow1^1A_g$ is parity forbidden.

Although Tanizaki's calculation was including only π-

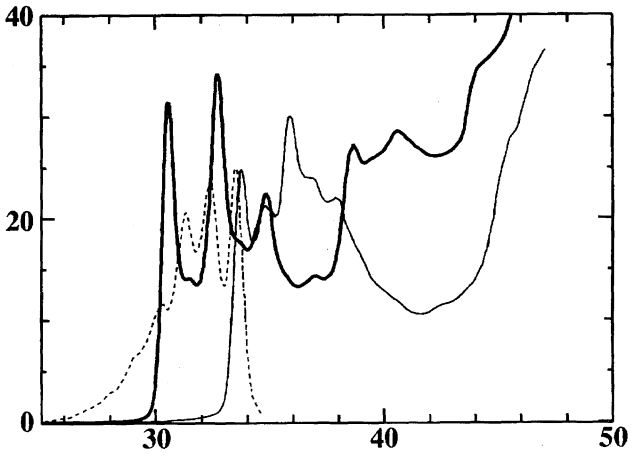

Fig. 2. Absorption spectra of DPA (thin line) and DPB (thick line) in cyclohexane. Fluorescence spectrum of DPA (broken line) excited at 295 nm is also shown in the figure. Fluorescence spectrum was corrected for the sensitivity of the apparatus.

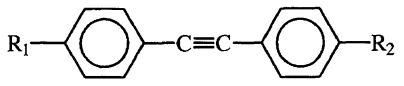

Fig. 1. Molecular structure of DPA derivatives.

R_1	R_2	
H–	H–	DPA
H–	OH–	OH–DPA
H–	Cl–	Cl–DPA
H–	NH_2–	AM–DPA
H–	$(CH_3)_2N$–	DA–DPA
H–	CH_3O–	MO–DPA
CH_3O–	CH_3O–	DM–DPA
H–	CH_3OOC–	CH_3OOC–DPA
H–	NO_2–	NO–DPA
H–	CH_3CO–	CH_3CO–DPA
H–	CN–	CN–DPA
CN–	NH_2–	AMCN–DPA
CN–	$(CH_3)_2N$–	DACN–DPA
CN–	CH_3S–	MTCN–DPA

orbitals perpendicular to the molecular plane, the semi-empirical MO calculations including σ-orbitals were later carried out and the character and the energetic ordering of the low-lying electronically excited singlet states of DPA were discussed.[41,42] Gutmann et al.[41] used the CNDO/S-CI method and performed the calculation at the geometries obtained from both the X-ray data[32,33] and the AM1 calculations. In this calculation they included 400 energy-selected singly- and doubly-excited configurations. Ferrante et al.[42] used the INDO-S method at the AM1-optimized geometry of the ground electronic state. The calculation included 200 energy-selected singly and doubly excited configurations for the singlet state and 300 for the triplet states. The results of the MO calculations are listed in Table 1.

All of these calculations predict that the lowest excited singlet state to which a one-photon transition is allowed from the ground state is 1^1B_{1u}. The $1^1B_{1u}\leftarrow 1^1A_g$ transition is strongly allowed and long-axis polarized, which is in agreement with polarization measurements performed on single-crystal[47] and stretched sheets.[46,48] The 1^1B_{2u} state which is weakly one-photon allowed from the ground state is not the lowest excited singlet state but it is located near the 1^1B_{1u} state. Gutmann et al. and Ferannte et al. calculated that a 2^1A_g state was 7000—9000 cm^{-1} higher than the 1^1B_{1u} state. The lowest excited singlet state with *g*-symmetry was calculated to be the 1^1B_{3g} state.

Changing the C≡C bond length, Ferante et al. estimated the equilibrium bond lengths for several states.[42] The values so obtained are 1.200 A in the ground state, 1.245 A in the 1^1B_{1u} state, and 1.280 A in the 1^1A_u state. According to their calculations, the 1^1A_u state, which is one- and two-photon forbidden from the ground state, is the lowest excited singlet state but the 1^1B_{1u} state is the lowest excited singlet state at the ground state geometry. At the present stage of investigation, it seems to be impossible to obtain optimized geometries of the excited singlet states by using full-CI MO calculations.

Okuyama et al. measured the fluorescence excitation and two-photon resonant four-photon ionization spectra in the supersonic free jet and confirmed the presence of three excited singlet states in the first absorption band region.[40] Following Tanizaki's calculation,[46] they assigned the most intense band in the fluorescence excitation spectra, which appears at 35248 cm^{-1} and is accompanied by a short progression of about 96 cm^{-1}, to the origin of the $1^1B_{1u}\leftarrow 1^1A_g$ transition. Another short progression with a 85 cm^{-1} interval starts from 35051 cm^{-1}, which is assigned to the false origin of the 1^1B_{2u} band. The two-photon resonant four-photon ionization spectrum, which starts at 34960 cm^{-1} and shows the mutual exclusion, is also observed in the supersonic jet. No observed bands of the two-photon resonant spectrum coincide in the spectral position of the one-photon absorption band. Moreover, the vibrational structure is well explained in terms of the vibrations with an a_g symmetry. These results strongly indicate that the two-photon resonant band is ascribed to the state with *g*-symmetry. They tentatively assigned it to the 2^1A_g state.

The 96 and 85 cm^{-1} is considered to be two quanta of the torsional vibration about the triple bond in the 1^1B_{1u} and 1^1B_{2u} states, respectively. Measuring the dispersed fluorescence spectra from the 1^1B_{1u} and 1^1B_{2u} states, they evaluated the barrier height of the internal rotation of the phenyl group in the S_0 state. The obtained value is 202 cm^{-1}, which is much larger than that of dimethylacetylene (< 4 cm^{-1}).[49] The large barrier of the torsional mode is ascribed to the strong π-conjugation throughout the molecule. By using the same rotational constant and the same potential function as those of the S_0 state, they estimated the barrier heights in the 1^1B_{1u}, 1^1B_{2u}, and 2^1A_g states to be 1590±50, 1280±50, and 1080±45 cm^{-1}, respectively.[50] From these results we realized that the π-conjugation throughout the molecule is stronger in the excited singlet states than that in the S_0 state and the strength of the π-conjugation decreases in the order: $^1B_{1u}$, $^1B_{2u}$, and 2^1A_g.

From the results of the dispersed fluorescence and one- and two-photon fluorescence excitation spectral measurements in low temperature matrices, Gutmann et al. suggests that the level ordering in the condensed phase is different from that in the gas phase. The S_1 state of DPA has a B_{1u} symmetry and the two-photon absorption is due to the vibronic coupling between 1^1B_{1u} and 1^1B_{3g} via b_{2u} modes. It is important to note here that two excited singlet states (1^1B_{1u} and 1^1B_{2u}) emit

Table 1. Calculated Excitation Energy (ΔE/cm^{-1}), Oscillator Strength (f), Two-Photon Cross Section for Two Equally Linear Polarized Photons of Equal Energy (δ), and Two-Photon Polarization of DPA

	Tanizaki[a]		Gutmann (X-ray)[b]				Gutmann (AM1)[b]				Ferrante[c]			
	ΔE	f	ΔE	f	δ	Ω	ΔE	f	δ	Ω	ΔE	f	δ	Ω
1^1B_{1u}	32051	1.42	37811	0.49			34870	0.58			33360	0.679		
1^1B_{2u}	33784	0.0	41560	0.01			38964	0.01			34618	0.006		
1^1B_{3g}			41566		1.1	1.50	38969		1.4	1.50	34642		1.75	1.50
1^1A_u			37489				35076				34779			
2^1A_g	33784		45798		9.7	0.73	43306		17.2	0.75	40305		24.61	0.76
2^1A_u			43671				42202				42417			
2^1B_{1u}	45249	0.56	48170	0.02			46552	0.01			44528	0.067		
3^1A_g	43290		53702		197.0	0.74	49327		191.9	0.74	45350		147.19	0.76

a) Ref. 39 b) Ref. 31 c) Ref. 32.

fluorescence in the gas phase, while only one fluorescence (1^1B_{1u}) is detected in the condensed phase.

Neither the jet cooled fluorescence excitation spectrum nor the one-photon resonant two-photon ionization spectrum is observed in the frequency region higher than 36000 cm^{-1}. The drastic decrease in the fluorescence quantum yield with increasing excitation energy was thought to be an indication of the existence of an ultrafast relaxation process in the higher energy region.[40] On the contrary, such a significant decrease is not observed in the two-photon resonant spectrum. The different behavior of the one- and two-photon resonant spectra should be important to make the relaxation mechanism clear.

A gradual decrease of the fluorescence yield with increasing excitation energy is observed in the solution phase at room temperature.[39] On the other hand, the fluorescence and its excitation spectra in the low temperature matrices was reported to exhibit an excellent mirror symmetric relation. A broadening of the fluorescence excitation spectra is also observed above an excess energy of about 1000 cm^{-1}, which suggests the increasing coupling between the two electronic states with increasing excitation energy.[41]

2 Decay Process of the Low-Lying Excited Singlet States of DPA

Picosecond transient absorption measurements of DPA were performed in nonpolar solvents.[38,39] Figure 3 shows the time-resolved absorption spectra of DPA in hexane at room temperature excited with a 295-nm dye laser pulse. Immediately after the laser pulse excitation a sharp absorption band appears at 500 nm. The band is rapidly replaced with the bands peaked at 435 and 700 nm with increasing delay time. At delay times longer than 500 ps, the spectrum

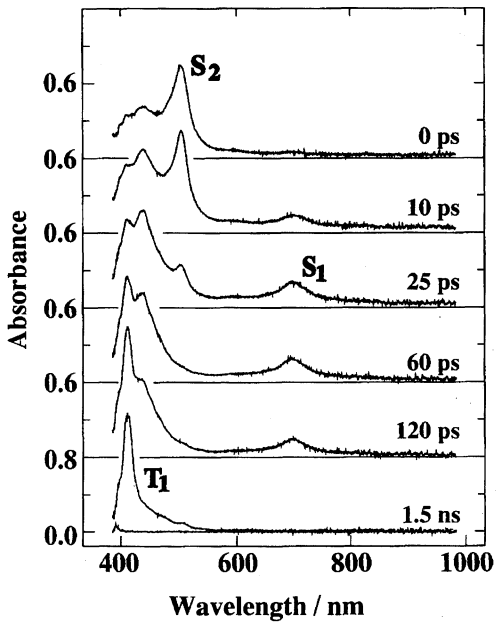

Fig. 3. Picosecond time-resolved absorption spectra of DPA in hexane at room temperature excited with a 295-nm dye laser pulse.

is characterized by a sharp and intense 415-nm band, which is assigned to the $T_n \leftarrow T_1$ transition of DPA.[51] At room temperature, the lifetime of the 500-nm band was estimated to be about 8 ps which agreed with the fluorescence lifetime. Later, a slightly shorter lifetime was reported by using femtosecond spectroscopy.[52] The lifetime of the 435 and 700-nm bands is about 200 ps, which is in good agreement with the rise time of the T_1 state. No fluorescence with a decay time of 200 ps is detected.

From the rise and decay times of the transient absorption spectra, the excitation and relaxation sequence

$$S_0 \xrightarrow{h\nu} X \longrightarrow Y \longrightarrow T_1$$

is established, where the species X gives the 500-nm band and the species Y gives the 435 and 700-nm bands. Because of the coincidence with the decay time of X and the fluorescence lifetime, X must be the fluorescence state of DPA. From the mirror symmetric relation of the absorption and fluorescence spectra, it can be deduced that X is the 1^1B_{1u} state, which is responsible for most of the intensity of the first absorption band. The species Y is the precursor of the T_1 state and is assigned to the S_1 state; thus the species X is the S_2 state.

Since the triplet formation is not observed in the short delay times, the $S_2 \rightarrow T_1$ intersystem crossing is not important at room temperature. A drastic temperature effect of the S_2 lifetime is found, while the S_1 state lifetime is almost temperature independent. At lower temperature than ca. 130 K the $S_2 \rightarrow S_1$ internal conversion is almost completely suppressed and the S_2 lifetime is as long as 1 ns. With decreasing temperature, the triplet yield decreases and the fluorescence yield increases. Because of the large energy gaps, the $S_2 \rightarrow S_0$ and $S_1 \rightarrow S_0$ internal conversions may be neglected. If we use the reported value of the fluorescence yield of 0.5 at 77 K,[53] the rate of the $S_2 \rightarrow T_1$ intersystem crossing is about 0.5 ns^{-1}. On the other hand, the $S_1 \rightarrow T_1$ intersystem crossing is as fast as 5 ns^{-1}.

Various DPA derivatives were the subject of time-resolved studies concerned with the photophysical process in solution. The strongly temperature dependent $S_2 \rightarrow S_1$ internal conversion and fluorescence yield are observed for amino, chloro, hydroxy, and methoxy derivatives, while the fluorescence yields of dimethylamino, cyano, and CH_3OOC- derivatives are found to be almost temperature independent.[54,55] Figures 4 and 5 show the picosecond transient absorption spectra of the former and the latter groups, respectively. In Fig. 4, short-lived bands are observed around 500 nm. On the other hand, the 500-nm bands of the CN– and CH_3OOC- derivatives (Fig. 5) are much longer-lived than those of the former group and the bands around 700 nm are not observed. The lifetimes of the 500-nm band are 0.56 and 0.70 ns for CN– and CH_3OOC-, respectively, which are in good agreements with the fluorescence lifetimes. These results indicate that the S_1 state of the latter group is the 1^1B_{1u} state. The level ordering of the low-lying excited singlet states of the former group is the same as that of DPA, while the inversion of the level ordering occurs with the introduction of the CN– or

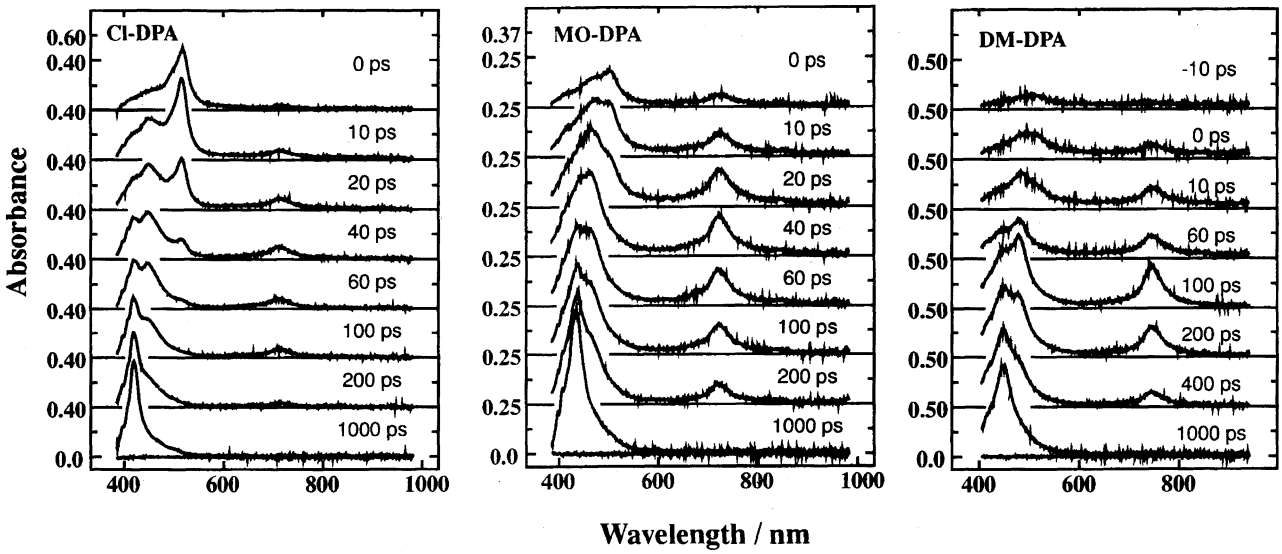

Fig. 4. Picosecond time-resolved absorption spectra of Cl–, MO–, and DM–DPA in hexane at room temperature excited with a 295-nm dye laser pulse.

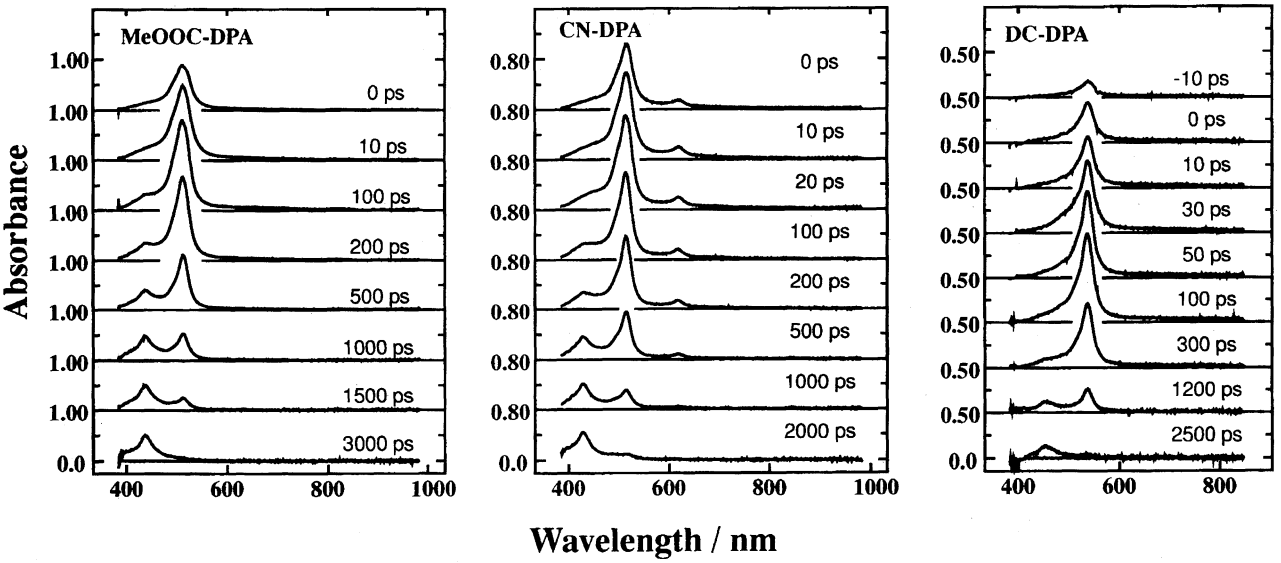

Fig. 5. Picosecond time-resolved absorption spectra of CH_3OOC–, CN–, and DC–DPA in hexane at room temperature excited with a 295-nm dye laser pulse.

CH_3OOC– group into the para-position of DPA. The intersystem crossing of CH_3CO–DPA and NO_2–DPA is so fast that the excited singlet state is not observed with a time resolution of about 10 ps.

The temperature dependence of the 1^1B_{1u} state lifetime of several DPA derivatives is displayed in Fig. 6. The lower the temperature, the longer the S_2 ($^1B_{1u}$) state lifetimes of MO–, OH–, and Cl–DPA are obtained, while the S_1 ($^1B_{1u}$) state of CN–DPA shows almost no temperature dependence. Except for CN–DPA, similar activation energies and the frequency factors are obtained. The temperature dependence of the S_2 lifetime of DPA should be determined by the $S_2 \rightarrow S_1$ internal conversion. In the case of CN– and CH_3OOC–DPA, of which the S_1 state is B_{1u}, the effective deactivation channels of the S_1 state is the temperature independent radiative process and the $S_1 \rightarrow T_1$ intersystem crossing. The excitation wavelength dependence of the fluorescence yield is not large for CN–DPA and the fluorescence yield is almost constant between 200 and 300 nm.

In order to study the role of the vibrational level density in the $S_2 \rightarrow S_1$ internal conversion, the results of the picosecond transient absorption measurements of DPA, methoxy–DPA, and DM–DPA were compared.[44] The transient absorption spectra ($S_n \leftarrow S_2$, $S_m \leftarrow S_1$, and $T_n \leftarrow T_1$) of these molecules are found to be quite similar to each other. In spite of the significant increase of the vibrational level density, methoxy substitution does not affect the frequency factor and the activation energy of the $S_2 \rightarrow S_1$ internal conversion. These results indicate that the total vibrational level density is not an important factor of the $S_2 \rightarrow S_1$ internal conversion of DPA in solution.

More detailed study on the dynamic behavior of the ex-

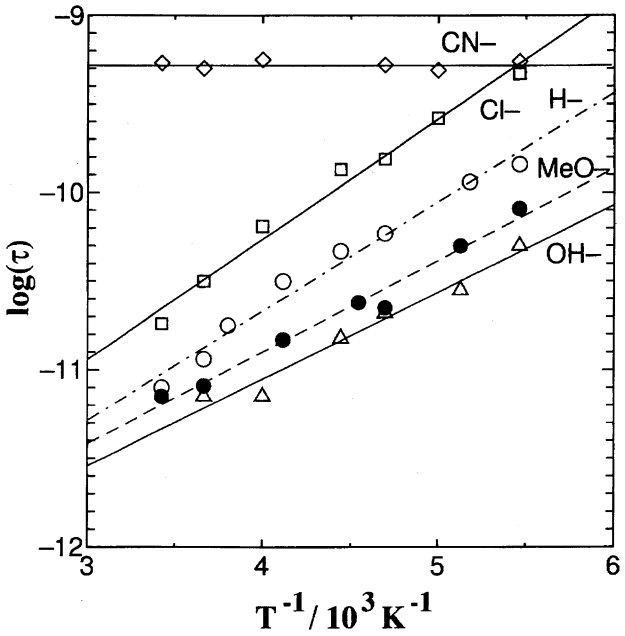

Fig. 6. Temperature dependence of the S_2 state lifetime of several DPA derivatives in hexane at room temperature.

cited singlet states was carried out for AM–DPA in non-polar solvents.[56] Figure 7 shows picosecond time resolved absorption spectra of AM–DPA in hexane at various temperatures. Although the $S_n \leftarrow S_2$, $S_n \leftarrow S_1$, and $T_n \leftarrow T_1$ absorption bands of AM–DPA are broader than those of DPA and appear around 500 nm, the decay processes revealed from the transient absorption measurements are similar to those of DPA. The photophysical processes of AM–DPA in hexane are summarized in Scheme 1. From the fluorescence and absorption spectra in the near UV region, the S_2 energy is estimated to be 30960 cm^{-1}, which is about 2600 cm^{-1} lower than that of DPA in the same solvent. A decay of the fluorescence is found to be bi-exponential. Since the intensity of the long-lived component decreases with decreasing temperature, the

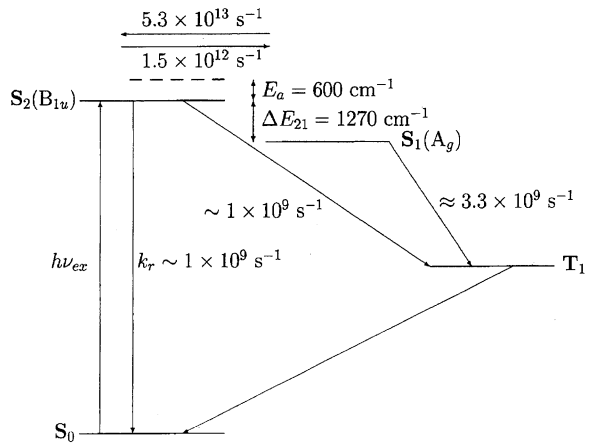

Scheme 1.

long-lived component is assigned to the delayed fluorescence which is due to thermal re-population of the S_2 state from the S_1 state. No S_1 fluorescence is observed.

The energy gap between the S_1 and S_2 states is estimated from the temperature dependence of the fluorescence decay. The value so obtained is about 1270 cm^{-1}. From the Arrhenius plot of the S_2 lifetime, the activation energy of the $S_2 \rightarrow S_1$ internal conversion is obtained to be about 600 cm^{-1}, which is slightly smaller than that of DPA. The frequency factors of the $S_2 \rightarrow S_1$ and $S_2 \leftarrow S_1$ internal conversions are evaluated to be 1.5×10^{12} and 5.3×10^{13} s^{-1}, respectively. The large frequency factor of the reverse process is responsible for the high yield of the delayed $S_2 \rightarrow S_0$ fluorescence and is characteristic of AM–DPA. The delayed S_2 fluorescence is not detected for DPA. The lifetime of the S_1 state may be determined by the $S_1 \rightarrow T_1$ intersystem crossing and is about 300 ps; it's temperature dependence seems to be small.

DA–DPA appears to show different photophysical behavior from DPA and AM–DPA.[55] As shown in Fig. 8, the transient absorption spectra of DA–DPA in hexane measured at 298 (a) and 180 K (b) are similar to each other. The 830-nm

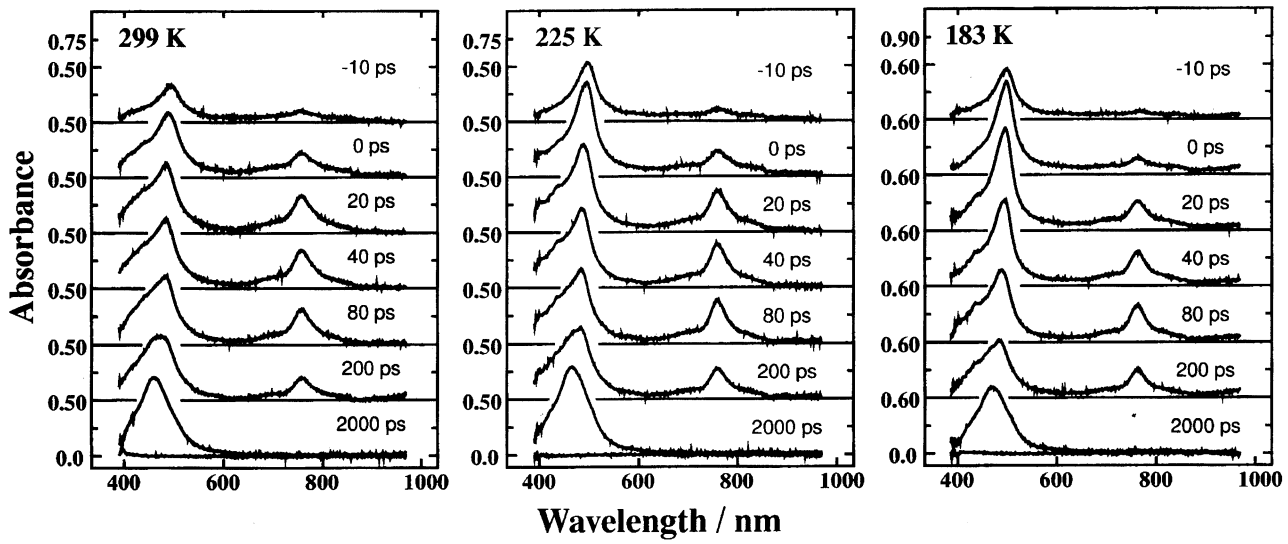

Fig. 7. Picosecond time-resolved absorption spectra of AM–DPA in hexane at 299, 225, and 183 K excited with a 295-nm dye laser pulse.

band is assigned to the $S_n \leftarrow S_1$ transition, of which the rise time coincides with a decay time of the short lived component observed at 530 nm. Since the rise time of the 830-nm band does not show strong temperature dependence, the activation energy of the $S_2 \rightarrow S_1$ internal conversion is expected to be much smaller than that of DPA.

Fluorescence decay curve of DA–DPA in hexane at 300 K is not single exponential but it can be analyzed as a bi-exponential function with the lifetimes of 435 and ca. 20 ps. The long-lived component should be due to the delayed fluorescence; the pre-exponential factor of the long-lived component is similar to that of the short-lived one. The ratio of the pre-exponential factors is found to be almost temperature independent, which suggests the accidental degeneracy of the S_1 and S_2 states. The fluorescence yield of DA–DPA in hexane excited at 300 nm is about 0.2, which is more than one order of magnitude larger than that of DPA and AM–DPA.

We can summarize the photophysical process of DPA derivatives as follows: 1) The fluorescence state of the DPA derivatives is the 1^1B_{1u} state. 2) The 1^1B_{1u} state is the S_2 state in many DPA derivatives except for CN– and CH_3OOC–. 3) The DPA derivatives of which the S_2 state has a B_{1u} symmetry show the strong temperature dependence of the S_2 state lifetime and the excitation wavelength dependence of the fluorescence yield. 4) Neither the distinct temperature dependence of the S_2 lifetime nor the excitation wavelength dependence of the fluorescence yield is observed for CN–DPA. 5) The S_2–S_1 energy gap of the DPA derivatives in solution seems to be small (1270 cm^{-1} for AM–DPA and ca. 0 for DA–DPA). 6) The total vibrational level density is not an important factor of the $S_2 \rightarrow S_1$ internal conversion.

3 Decay Process of the Low-Lying Excited Singlet States of DPB

The dynamic behavior of the S_2 state of DPB derivatives was studied by using femtosecond transient absorption measurement techniques.[44] Figure 9(a) shows the picosecond transient absorption spectra of DPB in cyclohexane. The intensities of the 780-nm band and the shoulder around 530 nm decreases rapidly with increasing delay time after the laser pulse excitation, while the intensity of the 445-nm band increases. The rise time of the 445-nm band is 25±10 ps and the decay time of the 565 and 780-nm bands is 30±8 ps. The long-lived 445-nm band is assigned to the $T_n \leftarrow T_1$ transition of DPB,[57] while the 780 nm band and the shoulder around 530 nm is assigned to the $S_n \leftarrow S_1$ transition. As shown in Fig. 9(b), the dynamic behavior of DM–DPB is similar to that of DPB; the $S_n \leftarrow S_1$ bands at 545 and 840 nm and the sharp $T_n \leftarrow T_1$ band at 475 nm are observed. The S_1 state lifetimes of DM–DPB and MO–DPB are 190±35 and 52±15 ps, respectively.

If the first absorption band around 330 nm in Fig. 2 is due to the S_1 state of DPB, the fluorescence yield should be as large as $\tau(S_1)/\tau_r \approx 0.03$. In the same manner, the fluorescence yield of about 0.2 is expected for DM–DPB. The failure to detect any fluorescence of these compounds implies that the major part of the first absorption band is not due to the $S_1 \leftarrow S_0$ transition. One-photon transition probability between the S_1 and S_0 states should be significantly smaller than that of the first absorption band. The situation seems to be quite similar to that of DPA.

As shown in Fig. 10(a), we observed a short-lived transient absorption band of DM–DPB around 430 nm. The decay curve shown in Fig. 10(b) is fitted to the double exponential function and the decay time of the short-lived component is estimated to be 680±120 fs. The rising part of the transient

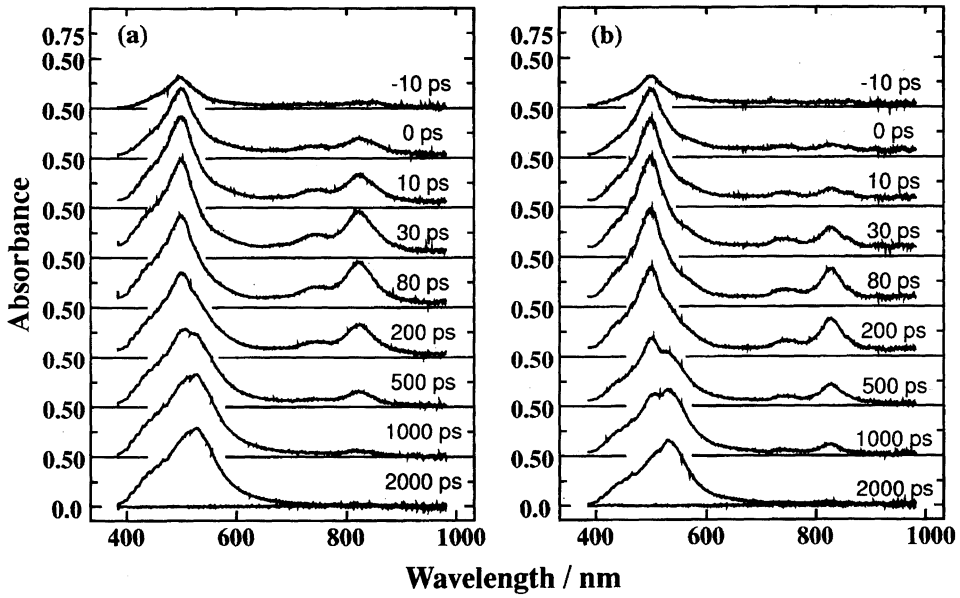

Fig. 8. Picosecond time-resolved absorption spectra of DA–DPA in hexane at (a) 298 and (b) 180 K excited with a 295-nm dye laser pulse.

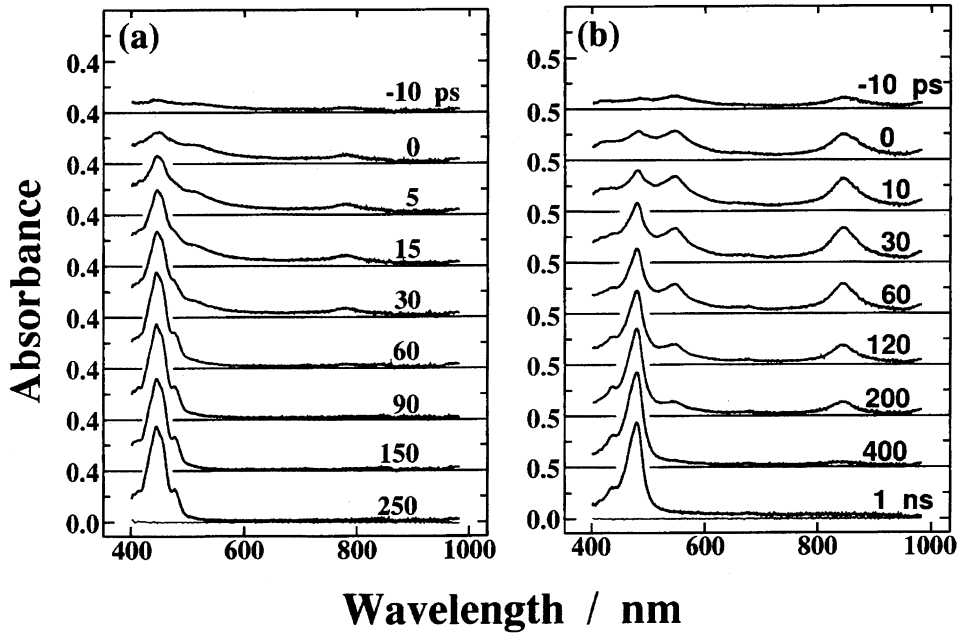

Fig. 9. Picosecond time resolved absorption spectra of (a) DPB and (b) DM–DPB in cyclohexane. Delay times after the laser pulse excitation are indicated in the figure.

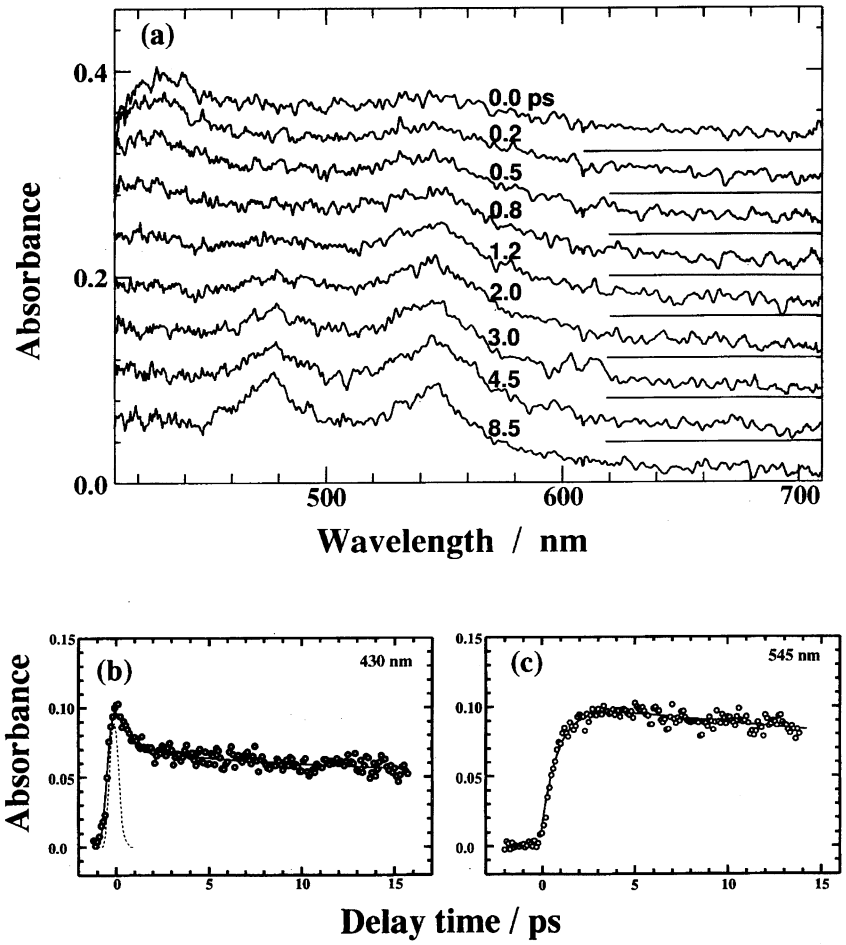

Fig. 10. Femtosecond time resolved absorption spectra and the time dependence of the transient absorbance of DM–DPB ((b) 480 and (c) 545 nm) in cyclohexane.

absorbance monitored at 545 nm (Fig. 10(c)) consists of a small portion of the instrumentally limited component and the exponentially rising component with a time constant of 640±150 fs. Because of the agreement between the decay time of the 430-nm band and the rise time of the 545-nm band, the 430 nm band can be assigned to the S_2 state of DM–DPB. The photophysical process of DPB and MO–DPB is similar to that of DM–DPB and their S_2 lifetimes are estimated to be about 600 fs.

As we mentioned, the introduction of the cyano groups to DPA results in the level inversion of the S_2 and S_1 states and only the S_1 (B_{1u}) state is observed by the fluorescence and transient absorption measurements. The level inversion seems to occur in DC–DPB, but both the S_1 and S_2 states of DC–DPB are observed by transient absorption measurements.[58] The temperature effect of the picosecond time-resolved absorption spectra is shown in Fig. 11. The band around 480 nm is assigned to the $T_n \leftarrow T_1$ absorption. The intensity ratio of the 570 and 630-nm bands, of which the decay times agree with the rise time of the triplet band (about 70 ps at 295 K), decreases with decreasing temperature. The rise time of the 570-nm band is about 2 ps and a decaying component of the 630-nm band with a similar time constant is observed. From these results, the 570 and 630 nm bands are assigned to the S_2 and S_1 states, respectively. Therefore we can conclude that the introduction of CN–groups leads to the level inversion of the lowest excited singlet states of DPB. Moreover the thermal re-population of the S_2 state is observed. The sum of the $S_2 \rightarrow S_1$ and $S_2 \leftarrow S_1$ internal conversion rates at room temperature is about 5×10^{11} s^{-1}, which is one order of magnitude smaller than the $S_2 \rightarrow S_1$ internal conversion rate of DPB and DM–DPB.

4 Decay Process of the Low-Lying Excited Singlet States of Diphenylpolyenes

Since many diphenylpolyenes exhibit dual fluorescence,[26] the S_2–S_1 energy gap of diphenylpolyenes in solution is available and we can investigate the correlation between the decay process and the energy gap. The S_2–S_1 gap, which is determined from the energy difference between the 0–0 maxima of the 1^1B_u absorption and the 2^1A_g fluorescence, is reported to increase with increasing chain length from about 1600 cm^{-1} for 1,6-diphenyl-1,3,5-hexatriene to 4800 cm^{-1} for 1,14-diphenyl-1,3,5,7,9,11,13-tetradecaheptaene.[59] In hexane at 4.2 K, the energy gap of 1,6-diphenyl-1,3,5-hexatriene is 786 cm^{-1}.[60] Investigations of the energy gap dependence must be important for the elucidation of the photophysical properties and the characters of the low lying excited singlet states. Moreover such studies should help to shed light on the dynamic behavior of the S_2 state of DPA derivatives, because the electronic structures of DPA derivatives are known to have some similarity with those of diphenylpolyenes.

Yee et al. measured femtosecond transient absorption spectra of 1,4-diphenyl-1,3-butadiene, 1,6-diphenyl-1,3,5-hexatriene, and 1,8-diphenyl-1,3,5,7-octatetraene in several nonpolar solvents at room temperature.[27] They excited the sample with the 390-nm laser pulse and observed the $S_n \leftarrow S_2$ absorption in the red region. The S_2 state lifetimes were evaluated from the rapidly decaying component of the transient absorbance monitored at 780 nm. The values so obtained for 1,8-diphenyl-1,3,5,7-octatetraene are 570, 600, and 470 fs in cyclohexane, dodecane, and octane, respectively. A short-lived component with the similar decay time is observed for 1,6-diphenyl-1,3,5-hexatriene, while no comparable fast decaying component is detected for 1,4-diphenyl-1,3-buta-

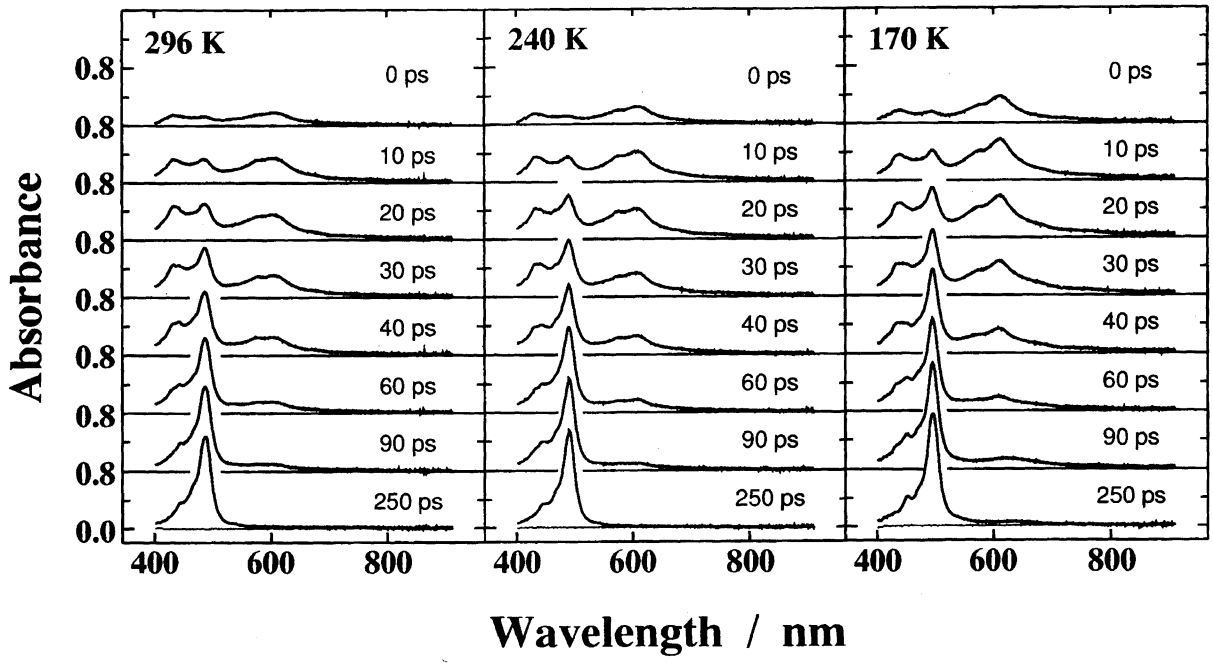

Fig. 11. Picosecond time resolved absorption spectra of DC–DPB in THF at 296, 240, and 170 K. Delay times after the laser pulse excitation were indicated in the figure.

diene.

Fluorescence lifetimes of *all trans*-diphenylpolyenes from 1,6-diphenyl-1,3,5-hexatriene ($N = 3$) to 1,14-diphenyl-1,3,5,7,9,11,13-tetradecaheptaene ($N = 7$) in solution were measured by Bachilo et al.[59] Closed circles in Fig. 12 show the rate constants of the $S_1 \rightarrow S_0$ internal conversion,[59] while open circles show the decay rates of the S_2 state.[61] Since the S_2–S_0 gap is large, it is reasonable to consider that the $S_2 \rightarrow S_0$ internal conversion is negligible and that the S_2 lifetime is essentially determined by the $S_2 \rightarrow S_1$ internal conversion. In contrast to the large energy gap dependence of the $S_1 \rightarrow S_0$ internal conversion,[59] the $S_2 \rightarrow S_1$ internal conversion is found to be almost constant for $N = 3$–7.[61]

The $S_1 \rightarrow S_0$ internal conversion rates are reported to follow the energy gap law of

$$\ln k(\Delta E) = \frac{\alpha - \gamma \Delta E}{h\nu}, \tag{4}$$

where ΔE stands for the S_1–S_0 energy gap and ν is the effective vibrational frequency. In Eq. 4, a weak $(\Delta E)^{-1/2}$ dependence included in Eq. 1 is neglected. The parameter α can be treated as a constant and γ is almost unity for polyenes. From the slope of the straight line in Fig. 12, ν is estimated to be 1070 cm^{-1}, which suggests that the C–C and C=C stretching modes are important as accepting modes of the $S_1 \rightarrow S_0$ internal conversion and that the high frequency C–H stretching mode is not effective.[59]

Within the framework of Born–Oppenhimer approximation, the transition probability of the radiationless transition can be factorized into an electronic integral and a vibrational overlap integral (Franck–Condon factor). Since Eq. 4 holds for the $S_1 \rightarrow S_0$ internal conversion, the N-dependence of the electronic integrals seems to be small. If the electronic integrals of the $S_2 \rightarrow S_1$ internal conversion do not show strong

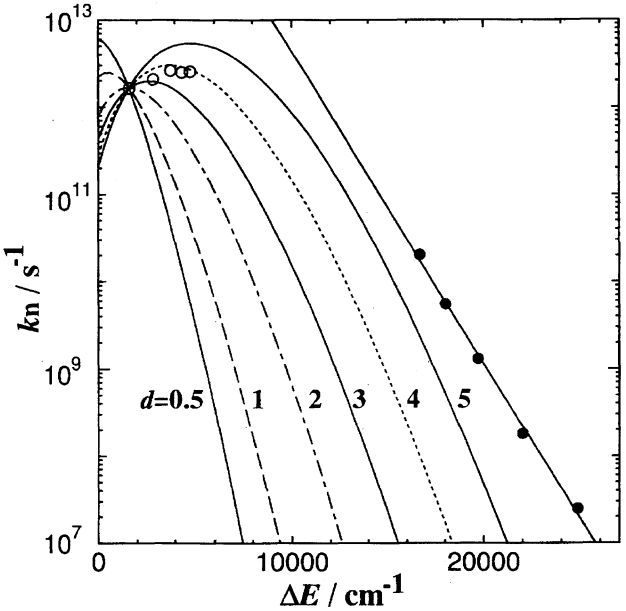

Fig. 12. Energy gap dependence of the S_2 lifetime (open circles) and the reported $S_1 \rightarrow S_0$ internal conversion rate of α, ω-diphenylpolyenes (closed circles).

N-dependence and the accepting mode of the $S_2 \rightarrow S_1$ internal conversion is a displaced but undistorted harmonic oscillator, the rate constant of the $S_2 \rightarrow S_1$ internal conversion is proportional to the Franck–Condon factor, which can be given as

$$|< v_n \mid v_0 >|^2 = \frac{e^{-\delta} \cdot \delta^n}{n!}, \tag{5}$$

where we assumed that the accepting mode is not excited in the S_2 state and n quanta of the accepting mode are excited in the S_1 state. The normalized displacement between the initial and final states is $\delta = K\Delta Q^2/(2h\nu)$, where K and ΔQ stand for the force constant and the difference in the equilibrium position of the accepting mode. From the experimental results, we cannot determine which mode is the accepting mode of the $S_2 \rightarrow S_1$ internal conversion. Assuming that the accepting mode has a frequency of $\omega = 1070$ cm^{-1}, which is the same as the effective frequency for the $S_1 \rightarrow S_0$ internal conversion, we calculated the Franck–Condon factors for $\delta = 0.5$, 1, 2, 3, 4, and 5. The curves in Fig. 12 are normalized to pass through the experimental point of $N = 3$. Strong energy gap dependence can be expected for small δ. Large displacements of $\delta = 3$—4 seem to reproduce the experimental results. Since Eq. 5 depends on the vibrational quantum number, n, but the frequency does not appear in the equation, we can expect the smaller energy gap dependence if the accepting mode has higher frequency.

5 $S_2 \rightarrow S_1$ Internal Conversion of DPA, DPB, and Diphenylpolyenes

As we mentioned, there are contradictions of the assignments of the low-lying excited singlet states of DPA. It is necessary to solve this problem before starting discussion of the mechanism of the $S_2 \rightarrow S_1$ internal conversion. Because of the large radiative transition probability, the assignment of the S_2 (1^1B_{1u}) state is straightforward. The fluorescence properties of the excited singlet states revealed from the supersonic beam study[40] are quite helpful to assign the S_1 state in the condensed phase. Since the fluorescence from the $^1B_{2u}$ state is observed under the supersonic beam conditions, this state cannot be our S_1 state. The strict forbidden character of the S_1–S_0 one-photon transition suggests that the S_1 state has g-symmetry. The S_1 state may be either 2^1A_g or 1^1B_{3g} state.

Gutmann et al. tried to detect the two-photon fluorescence of DPA,[41] but the g-state was not observed in the lower energy region than the 1^1B_{1u} state. The reason of the failure of observing the S_1 state should be the nonfluorescent character of S_1. Our results are also consistent with the excitation energy dependence of the fluorescence yield. As we can recognize from the significant temperature dependence of the S_2 lifetime, acceleration of the $S_2 \rightarrow S_1$ internal conversion should be observed at the higher excitation energy. Due to the rapid vibrational relaxation, the excitation energy dependence of the fluorescence yield cannot be so significant in condensed phase as it is observed under the collision free conditions. In the supersonic jet, fluorescence is not observed for the vibronic levels with 800 cm^{-1} or higher excess energy in

the 1^1B_{1u} state. The threshold energy is similar to the activation energy of the $S_2 \rightarrow S_1$ internal conversion in solution phase. The major decay channel of the S_1 state is the intersystem crossing which does not show strong excess energy dependence. This can be the reason of the smaller excitation energy dependence of the two-photon resonant spectrum.

Although the radiationless transition of the aromatic molecules are usually classified as the weak coupling limit, Ferrante et al. thought that the $S_2 \rightarrow S_1$ internal conversion of DPA is in the strong coupling limit.[42] They also proposed that the internal conversion is a kind of chemical reaction along the C≡C stretching mode, which shows a large displacement in the S_1 and S_2 states. Their mechanism seems to explain the observed temperature effect very well, but we have to carefully consider the role of the vibrational modes in the internal conversion.

If the radiative lifetime of the S_1 state is similar to that of diphenylpolyenes, the S_1 fluorescence of DPA should be detectable. Nonfluorescent character of the S_1 state indicates that the vibronic coupling to borrow a radiative transition moment is not effective in the DPA derivatives. A rigid structure of DPA may be responsible for the strict mutual exclusion principle and prevents the S_1 state to emit fluorescence. The vibrational modes with a b_{1u} (b_{2u}) symmetry may be required for the intensity borrowing via the 1^1B_{1u}–2^1A_g (1^1B_{3g}) coupling. The same modes are expected to play as promoting modes of the $S_2 \rightarrow S_1$ internal conversion.

Unfortunately, we do not know much about the vibrational modes in the excited singlet states of DPA, therefore it is not possible to determine the promoting and accepting modes of the $S_2 \rightarrow S_1$ internal conversion at the present stage of investigation. It is reasonable to consider that C–H stretching modes cannot play an important role because a sum of the activation energy of $S_2 \rightarrow S_1$ internal conversion and S_2–S_1 energy gap of AM–DPA is about 1870 cm^{-1}, which is much smaller than the frequency of the C–H stretching modes. No deuterium isotope effect of the frequency factor and the activation energy of $S_2 \rightarrow S_1$ internal conversion is observed, either. Since the total vibrational level density do not affect the internal conversion rate, vibrational modes of lower than the S_2–S_1 energy gap cannot contribute to the internal conversion, either. Thus, the important vibrational mode to explain the large temperature effect of $S_2 \rightarrow S_1$ internal conversion should have the frequency of ca. 1000—2000 cm^{-1}. Because of the small energy gap, only $n = 0$ and 1 levels of this mode can play an important role in the internal conversion.

The S_2 state lifetime is as long as 1 ns at the lower temperature than 130 K, while the frequency factor of the $S_2 \rightarrow S_1$ internal conversion is close to 1×10^{13} s^{-1}.[38,54] These results suggest that the decay channel to $n = 1$ is almost three orders of magnitude faster than that to $n = 0$. If the mode is an accepting mode, the ratio of the Franck–Condon factor can be calculated as

$$|< v_1 \mid v_0 >|^2 \; / \; |< v_0 \mid v_0 >|^2 = \delta.$$

It is usually expected that a good accepting mode has a large displacement, δ, but it must be much less than 10^3. Therefore, it is difficult to rationalize the observed large difference of the decay rates in this manner.

On the other hand, promoting mode is not a totally symmetric mode and the displacement should be 0. Thus the large value can be expected for the ratio of

$$|< v_1 \mid \partial/\partial Q \mid v_0 >|^2 \; / \; |< v_0 \mid \partial/\partial Q \mid v_0 >|^2 \sim |< v_1 \mid v_1 >|^2 \; / \; |< v_0 \mid v_1 >|^2,$$

since $< v_0 | v_1 > = 0$ for the undisplaced vibration. The slow internal conversion of DC–DPB between the S_2 and S_1 states may be explained in the similar manner. On the contrary, the energy gap of DPB may be larger than the frequency of the promoting mode and the $S_2 \rightarrow S_1$ internal conversion does not show the activation energy.

MO calculation of DPA shows that the configuration which involves the localized non-bonding electron on the acetylene carbon is not important in the low-lying excited states.[42] It is predicted that the exceptionally large lowering of the bond order of the C≡C bond and the simultaneous increase of the bond order between acetylene carbon and phenyl carbon is accompanied by the electronic excitation from the S_0 state to some of the low lying excited singlet states. The reported frequency of the central C–C stretching in the S_1 state is lower than 1600 cm^{-1}, which is a typical value for the C–C double bond.[36,37] From these results we can expect that the bond to the phenyl ring shows the strong double-bond character in the S_1 state. Therefore the plausible structure of the S_1 state is not the stilbene-like bent form but it is the allene-like linear form, which will be consistent with the large torsional barrier height in the excited singlet states.[40]

6 Intramolecular Charge Separation of DPA Derivatives in Polar Solvents

Intramolecular charge separation of MTCN–DPA in various polar solvents was studied by using fluorescence measurement techniques.[29] A mirror symmetric relation of absorption (λ_{max} = 325 nm) and fluorescence spectra are observed in nonpolar solvents, while in polar solvents, a solvatochromic shift of the fluorescence is quite large (λ_{max} = 442 nm in acetonitrile; λ_{max} = 351 nm in hexane). Measuring the solvatochromic shifts of the fluorescence in polar solvents, Khundkar et al. estimated the dipole moment of the CS state to be 19 Debye larger than that of the S_0 state. By using the AM-1 calculation, the dipole moments of the S_0 and S_1 states in acetonitrile are obtained to be 4.5 and 21.5 Debye, respectively, while the S_1 state in nonpolar solvents is predicted to have a small dipole moment.[62]

Because of the large dipole moment in the S_1 state in polar solvents, a rigid molecular structure, and weak hydrogen bonding character of the cyano and methylthio groups, MTCN–DPA is expected to be a good probe of solvation dynamics in polar solvents.[63] The observed strong solvent dependence of the fluorescence lifetime of MTCN–DPA is considered to be the normal and inverted behavior of the

Marcus theory,[64] but their explanation is doubtful because they did not take account of the character of the final state. At least, there are two channels of the charge recombination which lead to the triplet and the ground state formation.

DACN–DPA was investigated by using picosecond transient absorption and fluorescence measurement techniques.[30] As shown in Fig. 13, fluorescence spectrum in hexane exhibits a mirror symmetric relation with its absorption spectrum, while a structureless broad fluorescence with a quite large solvatochromic shift is observed in polar solvents. The absorption spectrum shows only a little red shift and a slight broadening with increasing solvent polarity. These results indicate that the intramolecular charge separation occurs in polar solvents.

As shown in Fig. 14, the Stokes' shifts of the fluorescence in polar solvents appear to follow the Mataga–Lippert equation[65]

$$\nu_{abs} - \nu_{fl} = \frac{2(\Delta\mu)^2}{ha^3}\left(\frac{\epsilon_s - 1}{2\epsilon_s + 1} - \frac{n^2 - 1}{2n^2 + 1}\right),$$

where ν_{abs} and ν_{fl} denote frequency of the absorption and fluorescence maximum, respectively. $\Delta\mu$ is the magnitude of the difference in dipole moments between the S_0 and CS states, a is the radius of a spherical cavity containing the dipole. The static dielectric constant and the optical refractive index of the solvent are shown by ε_s and n, respectively. The observation of the linear relation suggests that $\Delta\mu$ is almost constant for aprotic solvents (open circles). If we assume that a is 6.4 Å, $\Delta\mu$ is obtained to be 31 Debye, which is much larger than the reported value of MTCN–DPA. The Stokes' shift in 1,4-dioxane (open square) significantly deviated from the straight line, which may be an indication of the large local dipole of 1,4-dioxane. In protic solvents (closed circles), the environment seems to be less polar than that expected from the dielectric constant.

Picosecond time resolved absorption spectra of DACN–DPA in various solvents are shown in Fig. 15. In

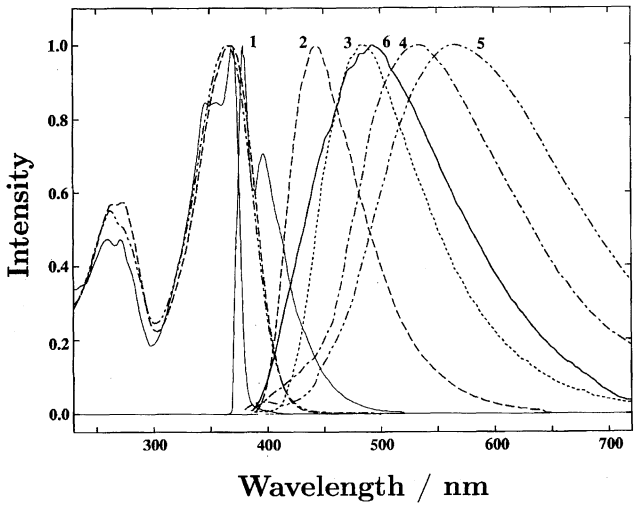

Fig. 13. Absorption and fluorescence spectra of DACN–DPA in 1: hexane, 2: diethyl ether, 3: tetrahydrofuran, 4: acetone, 5: acetonitrile, and 6: 1-butanol.

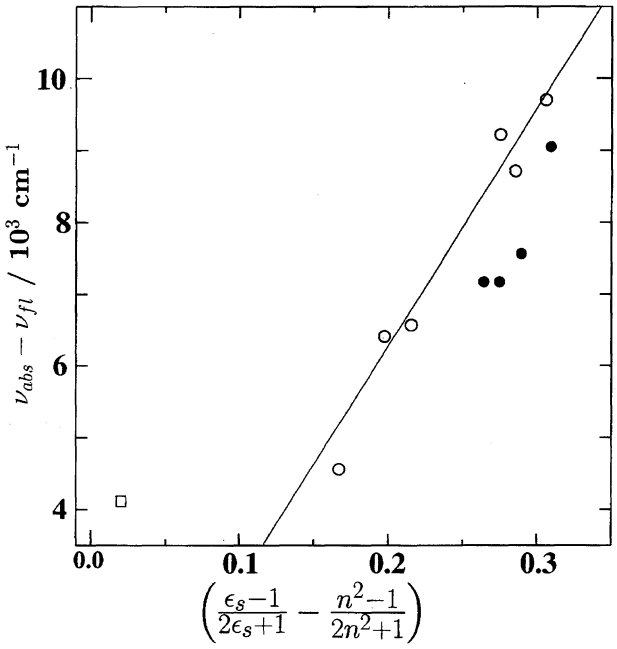

Fig. 14. Mataga–Lippert plot of DACN–DPA. Straight line shows the best fit to the Stokes' shift in aprotic polar solvents except 1,4-dioxane. Closed circles show the Stokes shift in alcohols.

hexane the 510-nm band (Fig. 15a), of which the lifetime is about 700 ps, is assigned to the $S_n \leftarrow S_1$ transition. In the longer delay time region, a broad $T_n \leftarrow T_1$ absorption band peaked at 640 nm is observed. In 1-butanol the 490-nm band (Fig. 15b), of which the lifetime is about 20 ps, can be ascribed to the locally excited singlet (S_1) state, while the transient absorption bands peaked around 430 and 690 nm are assigned to the CS state. The rise time of the 690-nm band agrees with the decay time of the S_1 state, while the decay of the 430- and 690-nm bands is about 460 ps which is in agreement with the fluorescence lifetime measured at a longer wavelength than 570 nm. Although the CS state is the lowest excited singlet state in polar solvents, we denote the locally excited singlet state whose electronic structure is similar to that of the fluorescence state in nonpolar solvents as S_1.

Transient absorption bands due to the CS state are observed at 690 (Fig. 15c) and 630 nm (Fig. 15d) and their lifetimes are about 2.8 and 0.9 ns in diethyl ether and acetonitrile, respectively. In diethyl ether, the sharp 480-nm band of which the decay is a double exponential with decay constants of ca. 15 ps and 2.7 ns is ascribed to the S_1 state. At 690 nm, a rapid rise (ca. 15 ps) and a decay (2.8 ns) of the transient absorbance are observed. These results indicate that the charge separation occurs from the S_1 state and the equilibrium between the CS state and the S_1 state is established in diethyl ether. Similar behavior is observed in 1,4-dioxane. In the highly polar solvents, a large stabilization of the CS state seems to prevent the back electron transfer to form the S_1 state. By using femtosecond transient absorption measurement techniques, the CS state band in acetonitrile is observed at 470 nm and the lifetime is evaluated to be about

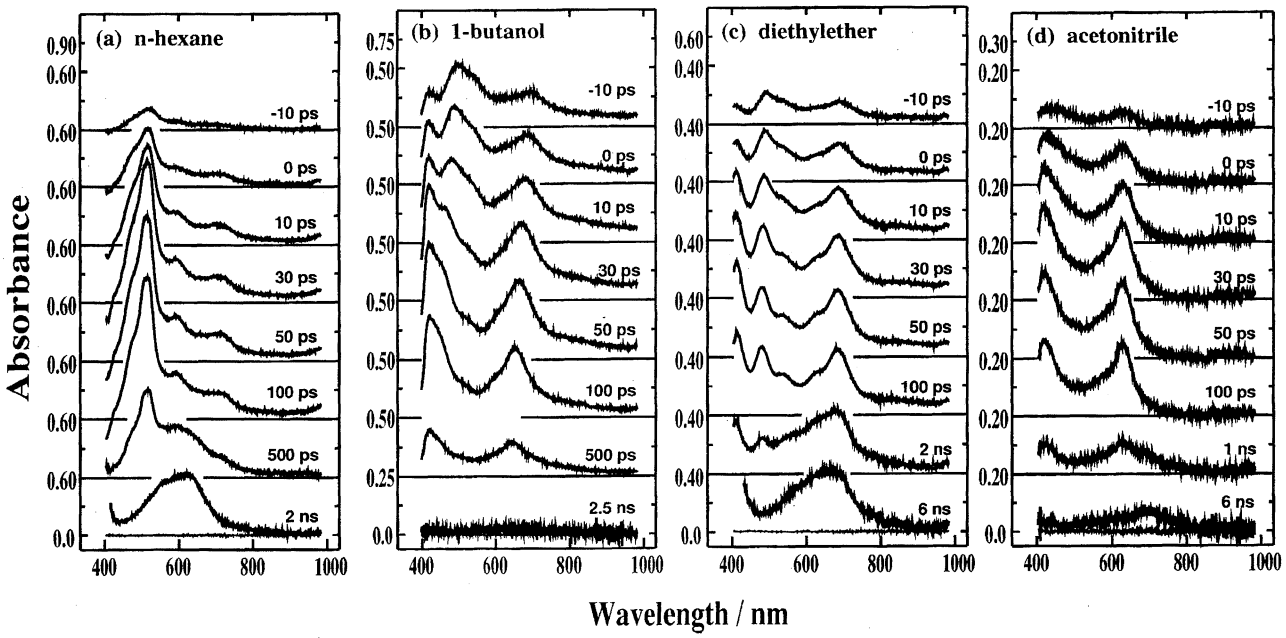

Fig. 15. Picosecond time resolved absorption spectra of DACN–DPA in various solvents. Delay times after the laser pulse excitation are shown in the figure.

3 ps.

At long delay times, the $T_n \leftarrow T_1$ absorption band peaked around 680-nm is observed. A significant decrease of the triplet yield and a shortening of the lifetimes of the CS state are observed in the order in diethyl ether, THF, acetonitrile, and 1-butanol. These results indicate that the major channel of the charge recombination both in highly polar solvents and in alcoholic solvents does not lead the triplet formation.

Since the peak position of the CS state band depends on the solvent polarity, it seems to be possible to use the spectral shift of the CS state band as an indicator of the local polarity of the solution. Figure 16 shows time dependence of peak position and full width at half maximum of the 690-nm band of DACN–DPA in 1-butanol. The spectral shift is observed only at shorter delay times than a few hundreds of picosecond and the peak energy at longer delay times is $\nu(\infty) \approx 15400$ cm^{-1}, while the band width, $\Delta\nu(t)$ is almost constant except for quite short delay times where the contribution of the $S_n \leftarrow S_1$ absorption band is not negligible. The absence of the significant change in the spectral band width with increasing delay time suggests that the progress in the solvation process in this time scale does not cause a significant change in the electronic structure of the CS state. A logarithmic plot of the spectral shift, $\nu(\infty) - \nu(t)$, against delay time exhibits a good linear relation and the relaxation time estimated from the slope is about 60 ps. In ethanol the relaxation time is found to be about 23 ps.

The intramolecular charge separation is also observed for AM– and DA–DPA which contain only an electron donating group.[66] Picosecond time resolved absorption spectra of AM–DPA in various solvents are shown in Fig. 17. Immediately after the excitation, the transient absorption band which can be ascribed to the S_2 state of AM–DPA appears at 480 (Fig. 17a) and 460 nm (Fig. 17b) in THF and acetonitrile,

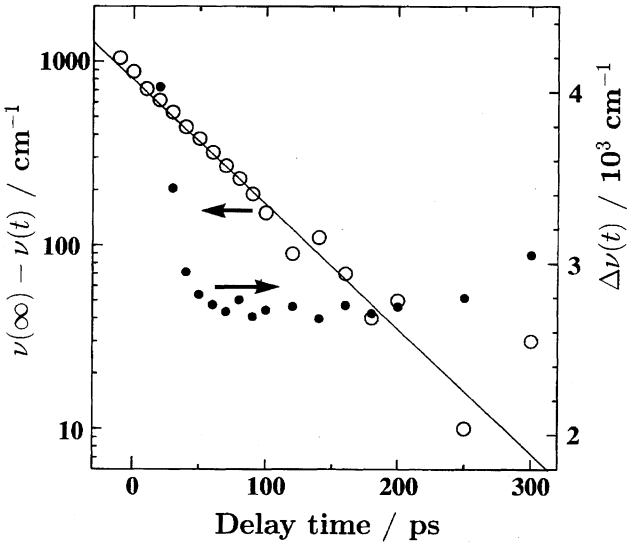

Fig. 16. Time dependence of the peak position (open circle) and a full width at half maximum (closed circle) of the 690-nm band of DACN–DPA in 1-butanol. Straight line shows the best fit to the spectral shift.

respectively. The S_2 band is rapidly replaced by the CS state band peaked at 660 and 640 nm in THF and acetonitrile, respectively. The long-lived $T_n \leftarrow T_1$ band is observed around 500 nm. The triplet yield decreases with increasing solvent dielectric constant of aprotic polar solvents. A quite similar behavior is observed for DA–DPA.

In 1-propanol immediately after the excitation, the $S_n \leftarrow S_2$ absorption band appears around 490 nm (Fig. 17c) and is rapidly replaced by the 660 and 790-nm bands. The 660-nm band is due to the CS state, while the 790-nm band can be ascribed to the $S_n \leftarrow S_1$ transition. These bands are short-lived and at the delay times longer than 200 ps, only a quite

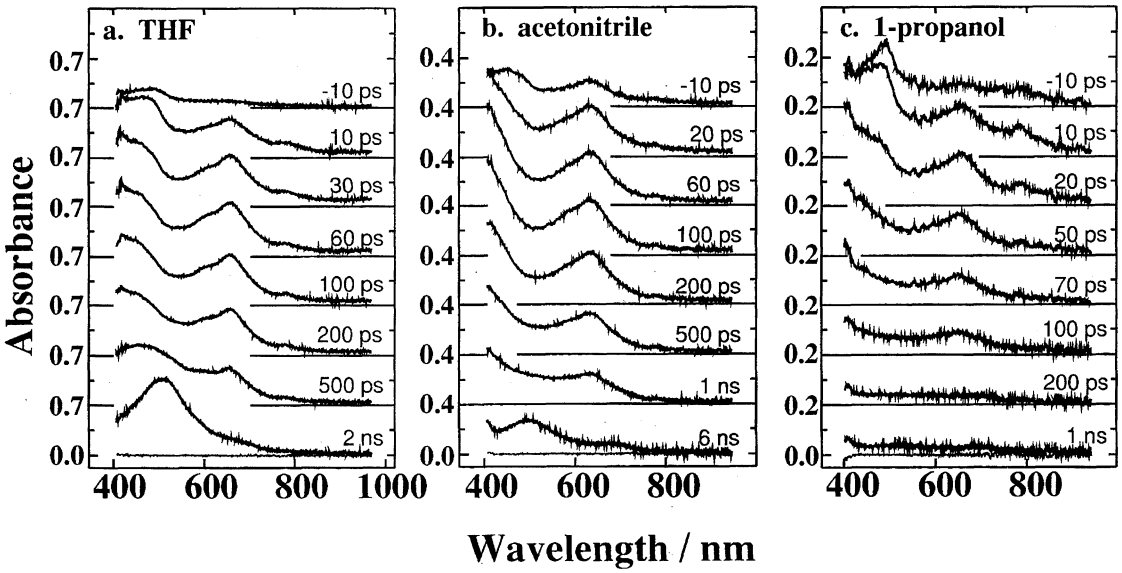

Fig. 17. Picosecond time resolved absorption spectra of AM–DPA in various polar solvents. Delay times after the laser pulse excitation are shown in the figure.

weak and broad transient absorption is observed. The $S_n \leftarrow S_1$ absorption is also observed in less polar aprotic solvents such as diethyl ether at shorter delay times. The decay times of the CS state of AM–DPA and DA–DPA in the various solvents are listed in Table 2.

In protic solvents, charge recombination is much faster than that in aprotic polar solvents. In methanol, little deuterium isotope effect in hydroxy group is observed. In normal alcohols, the lifetime seems to increase with increasing molecular size of solvent, while in 2-propanol the charge recombination is almost two times slower than that in 1-propanol. The lifetimes in formamide (FA) and *N*-methylformamide (NMF) are similar to that in 1-butanol, while in *N,N*-dimethylformamide (DMF) the CS state is quite long lived. These results clearly show that the enhancement of the charge recombination is due to a specific solute–solvent interaction in protic solvents.

One of the most plausible candidates of the specific solute–solvent interaction in protic solvents may be hydrogen bonding, but interaction (a) in Scheme 2 should not be the case because the enhancement of the charge recombination in the similar degree is observed for DA–DPA. Since the nitrogen atom in the amino group of the solute molecule is positively charged in the CS state, interaction (b) cannot be operative. On the contrary, the interaction between the nitrogen atom and the electron rich oxygen atom of the solvent molecule (interaction (c)) should play an important role. The interaction may cause the deformation of the amino group and result in the rapid charge recombination in protic solvents.

Table 2. Fluorescence Lifetimes of the Intramolecular Charge Separated State and Decay Times of the Transient Absorbance Monitored in the Red Region for AM–DPA and DA–DPA in Various Polar Solvents

Solvent	AM–DPA		DA–DPA	
	τ_f / ns	τ_d(CS) / ns	τ_f / ns	τ_d(CS) / ns
Acetonitrile	1.41	1.3±0.1	1.76	1.8±0.1
n-Propionitrile	1.51	1.5±0.3	1.92	2.3±0.3
n-Butyronitrile	1.6	1.4±0.2	2.5	2.4±0.4
THF	1.02	0.91±0.07	1.48	1.4±0.06
Diethyl ether	0.50	0.47±0.05	0.72	0.69±0.06
1,4-Dioxane	0.66	0.63±0.07	1.03	1.0±0.1
Methanol	< 0.06	1.6×10^{-2}	< 0.06	1.7×10^{-2}
Methanol-O-*d*	< 0.06	1.5×10^{-2}	< 0.06	1.7×10^{-2}
Ethanol	< 0.06	2.3×10^{-2}	< 0.06	2.7×10^{-2}
1-Propanol	< 0.06	$(2.9\pm0.3)\times10^{-2}$	< 0.06	$(3.2\pm0.3)\times10^{-2}$
2-Propanol	ca. 0.08	$(8.0\pm0.4)\times10^{-2}$	ca. 0.08	$(8.2\pm0.5)\times10^{-2}$
1-Butanol	< 0.06	$(4.7\pm0.3)\times10^{-2}$	< 0.06	$(5.2\pm0.3)\times10^{-2}$
DMF	1.3	1.3±0.2	2.1	2.2±0.3
NMF	ca. 0.07	$(5.8\pm0.5)\times10^{-2}$	ca. 0.08	$(8.4\pm0.7)\times10^{-2}$
FA	ca. 0.07	$(5.8\pm0.6)\times10^{-2}$	ca. 0.08	$(7.8\pm0.6)\times10^{-2}$

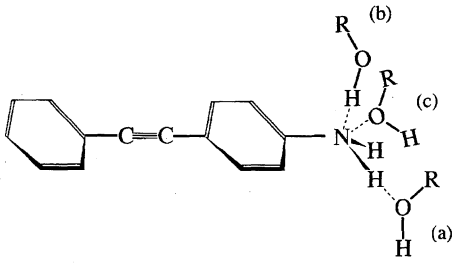

Scheme 2.

Although we may expect that DMF, which has carbonyl oxygen and almost the same dipole moment as NMF and FA, can interact with the amino group in a similar manner, the lifetime of the CS state does not show any shortening effect in DMF. Considering the microscopic structures of liquid,[67–69] we proposed that the competition between the solvent–solute and solvent–solvent interaction is important for the charge recombination. Interaction between the amino nitrogen atom of the solute molecule and the oxygen atom at the donor terminal of hydrogen-bonded solvent oligomer may be a mechanism of the significant enhancement of the charge recombination in protic solvents.

7 Concluding Remarks

A review of the photophysical and photochemical primary processes of DPA derivatives and related compounds exhibited curious properties of the low-lying excited singlet states. The most important property of the lowest excited singlet states, which was revealed from the picosecond and femtosecond transient absorption and fluorescence spectral measurements, is the strong temperature dependence of the $S_2 \rightarrow S_1$ internal conversion. The internal conversion requires the thermal activation and is almost completely suppressed at low temperatures. Since such a significant temperature effect is not observed for the radiationless transitions of other aromatic molecules, Ferrante et al. proposed that the process is a kind of chemical reaction.[42] We considered that such properties should be due to the small S_2–S_1 gap as well as the high frequency of the efficient promoting mode of the $S_2 \rightarrow S_1$ internal conversion. The high frequency promoting mode cannot be excited even in the final (S_1) state of the internal conversion without thermal assistance. DPB seems to have larger S_2–S_1 gap and does not show the strong temperature of the $S_2 \rightarrow S_1$ internal conversion. Introduction of cyano groups to DPB makes the energy gap smaller and results in the slower internal conversion.

The excitation energy dependence of the fluorescence yield is also important. The assignment of S_1 to the state with a *g*-symmetry seems to solve the contradictions except for the predictions of the MO calculations by Gutmann et al.[41] and Ferrante et al.[42] Our assignment can explain the significant decrease of the fluorescence yield in the gas phase with increasing excitation energy. Since the intersystem crossing from the S_1 state is one order of magnitude faster than that from the S_2 state, the triplet yield decreases with decreasing temperature.

In order to give more concrete substantiation of our mechanism and to elucidate the details of the $S_2 \rightarrow S_1$ internal conversion, high resolution spectroscopy of several DPA derivatives is required. Such studies must be able to handle nonfluorescent states. Several papers concerned with the Raman spectra of DPA in the excited states are available[34–37] but they are limited to DPA itself and the derivatives such as CN–DPA are not investigated.

The author would like to express his sincere thanks to Professor T. Okada, who has given invaluable advice and encouragement to the author to accomplish his research. Thanks are also due to Professor T. Nomoto, who has provided various compounds.

References

1 J. Jortner, S. A. Rice, and R. W. Hochstrasser, *Adv. Photochem.*, **7**, 149 (1969).
2 K. F. Freed, in "Radiationless Processes in Molecules and Condensed Phases,"ed by F. K. Fong, Springer-Verlag, Berlin (1976).
3 G. W. Robinson and R. P. Frosh, *J. Chem. Phys.*, **37**, 1962 (1962); *J. Chem. Phys.*, **38**, 1187 (1962).
4 Bixon and J. Jortner, *J. Chem. Phys.*, **48**, 715 (1968).
5 R. Englman and J. Jortner, *Mol. Phys.*, **18**, 145 (1970).
6 W. Siebrand, in "The Triplet State," ed by A. B. Zahlan, Cambridge University Press, London (1967).
7 C. S. Huang and E. C. Lim, *J. Chem. Phys.*, **62**, 3826 (1975).
8 M. Kasha, *Discuss. Faraday Soc.*, **9**, 14 (1950).
9 J. W. Sidman and M. S. McClure, *J. Chem. Phys.*, **24**, 757 (1956).
10 A. R. Lacy, R. G. Budy, G. Frank, and I. G. Ross, *J. Chem. Phys.*, **47**, 2199 (1967).
11 G. Binsch, E. Heilbronner, R. Jankow, and D. Schmidt, *Chem. Phys. Lett.*, **1**, 135 (1967).
12 M. Mahaney and J. R. Huber, *Chem. Phys.*, **9**, 371 (1975).
13 J. R. Huber and M. Mahaney, *Chem. Phys. Lett.*, **30**, 410 (1975).
14 R. Anderson, Jr., R. M. Hochstrasser, and H. J. Pownall, *Chem. Phys. Lett.*, **43**, 224 (1976).
15 A. R. Holzwarth, K. Razi Naqvi, and U. P. Wild, *Chem. Phys. Lett.*, **46**, 473 (1977).
16 B. S. Hudson and B. E. Kohler, *Chem. Phys. Lett.*, **14**, 299 (1972).
17 B. S. Hudson and B. E. Kohler, *J. Chem. Phys.*, **59**, 4984 (1973).
18 K. Shulten and M. Karplus, *Chem. Phys. Lett.*, **14**, 305 (1972).
19 B. S. Hudson and B. E. Kohler, *Annu. Rev. Phys. Chem.*, **25**, 437 (1974).
20 B. S. Hudson, B. E. Kohler, and K. Shulten, in "Excited States," ed by E. C. Lim, Academic Press, New York (1982), Vol. 6, p.1.
21 L. A. Heimbrook, B. E. Kohler, and T. A. Spiglanin, *Proc. Natl. Acad. Sci. U.S.A.*, **80**, 4580 (1983).
22 J. F. Shepanski, B. W. Leelan, and A. H. Zewail, *Chem. Phys. Lett.*, **103**, 9 (1983).
23 J. S. Horwitz, B. E. Kohler, and T. A. Spiglanin, *J. Chem. Phys.*, **83**, 2186 (1985).
24 S. P. Velsko and G. R. Fleming, *J. Chem. Phys.*, **76**, 3553 (1982).

25 R. A. Goldbeck, A. J. Twarowski, E. L. Russell, J. K. Rice, R. R. Birge, E. Switkes, and D. S. Kliger, *J. Phys. Chem.*, **77**, 3319 (1982).
26 T. Itoh and B. E. Kohler, *J. Phys. Chem.*, **91**, 1760 (1987).
27 W. A. Yee, R. H. O'Neil, J. W. Lewis, J. Z. Zhang, and D. S. Kliger, *Chem. Phys. Lett.*, **276**, 430 (1997).
28 J.-M. Viallet, F. Dupuy, R. Lapouyade, and C. Rulliere, *Chem. Phys. Lett.*, **222**, 571 (1994).
29 L. R. Khundkar, A. E. Stiegman, and J. W. Perry, *J. Phys. Chem.*, **94**, 1224 (1990).
30 Y. Hirata, T. Okada, and T. Nomoto, *Chem. Phys. Lett.*, **278**, 133 (1997).
31 Y. Hirata, Y. Kanemoto, T. Okada, and T. Nomoto, *J. Mol. Liq.*, **65/66**, 421 (1995).
32 A. Mavridis and I. Moustakali-Mavridis, *Acta Crystallogr., Sect. B*, **33B**, 3612 (1977).
33 A. A. Espiritu and J. G. White, *Z. Kristallogr.*, **147**, 177 (1978).
34 H. Hiura and H. Takahashi, *J. Phys. Chem.*, **96**, 8909 (1992).
35 A. Shimojima and H. Takahashi, *J. Phys. Chem.*, **97**, 9103 (1993).
36 T. Ishibashi and H. Hamaguchi, *Chem. Phys. Lett.*, **264**, 551 (1997).
37 T. Ishibashi and H. Hamaguchi, *J. Phys. Chem. A*, **102**, 2263 (1998).
38 Y. Hirata, T. Okada, N. Mataga, and T. Nomoto, in "VII-th International Symposium on Ultrafast Processes in Spectroscopy," Inst. Phys. Conf. Ser. 126, ed by A. Laubereau, IOP Publishing (1992), pp. 481—484.
39 Y. Hirata, T. Okada, N. Mataga, and T. Nomoto, *J. Phys. Chem.*, **96**, 6559 (1992).
40 K. Okuyama, T. Hasegawa, M. Itoh, and N. Mikami, *J. Phys. Chem.*, **88**, 1711 (1984).
41 M. Gutmann, M. Gudipati, P. Schönzart, and G. Hohlneicher, *J. Phys. Chem.*, **96**, 2433 (1992).
42 C. Ferrante, U. Kensy, and B. Dick, *J. Phys. Chem.*, **97**, 13457 (1993).
43 B. Keller, H. H. Hacker, and J. Brandmüller, *Indian J. Pure Appl. Phys.*, **9**, 903 (1971).
44 Y. Hirata, T. Okada, and T. Nomoto, *Chem. Phys. Lett.*, **293**, 371 (1998).
45 S. J. Strickler and R. A. Berg, *J. Chem. Phys.*, **37**, 814 (1962).
46 Y. Tanizaki, H. Inoue, T. Hoshi, and J. Shiraishi, *Z. Phys. Chem. (Munich)*, **74**, 45 (1971).
47 S. C. Chakravorty and S. C. Ganguly, *Z. Phys. Chem. (Munich)*, **72**, 34 (1970).
48 E. W. Thulstrup and J. Michl, *J. Am. Chem. Soc.*, **104**, 5594 (1982).
49 W. B. Olson and D. Papousek, *J. Mol. Spectrosc.*, **37**, 527 (1971).
50 K. Okuyama, M. C. R. Cockett, and K. Kimura, *Annu. Rev. Inst. Mol. Sci.*, Okazaki, Japan (1991), p. 85.
51 K. Ota, K. Murofushi, and T. Hoshi, *Tetrahedron Lett.*, **1974**, 1434.
52 D. Zimdars, R. S. Francis, C. Ferrante, and M. D. Fayer, *J. Chem. Phys.*, **106**, 7498 (1997).
53 V. F. Razumov, V. A. Sazhnikov, M. V. Alfimov, I. L. Kotlyarevskii, and S. F. Vasilevskii, *Izv. Akad. Nauk SSSR, Ser. Khim. (Engl. Trans.)*, **1979**, 329.
54 Y. Hirata, T. Okada, and T. Nomoto, *Chem. Phys. Lett.*, **209**, 397 (1993).
55 Y. Hirata, T. Okada, and T. Nomoto, *Chem. Phys. Lett.*, **257**, 513 (1996).
56 Y. Hirata, T. Okada, and T. Nomoto, *J. Phys. Chem.*, **97**, 9677 (1993).
57 C. Pasternak, M. A. Slifkin, and M. Shinitzky, *J. Chem. Phys.*, **68**, 2669 (1978).
58 Y. Hirata, T. Okada, and T. Nomoto, *Acta Phys. Ploonica A*, **94**, 627 (1998).
59 S. M. Bachilo, C. W. Spangler, and T. Gillbro, *Chem. Phys. Lett.*, **283**, 235 (1998).
60 A. N. Nikitina, N. A. Ponomareva, L. A. Yanovskaya, V. A. Dombrovskii, and V. F. Kucherov, *Opt. Spektrosk.*, **40**, 251 (1976).
61 Y. Hirata, H. Fukumoto, K. Mashima, K. Tani, and T. Okada, *Chem. Phys. Lett.*, in press.
62 A. Broo, *Chem. Phys.*, **183**, 85 (1994).
63 L. R. Kundkar, J. T. Bartlett, and M. Biswas, *J. Chem. Phys.*, **102**, 6456 (1995).
64 R. A. Marcus, *J. Chem. Phys.*, **24**, 966 (1956); *J. Phys. Chem.*, **67**, 853 and 2889 (1963).
65 N. Mataga and T. Kubota, "Molecular Interactions and Electronic Spectra," Dekker, New York (1970).
66 Y. Hirata, T. Okada, and T. Nomoto, *J. Phys. Chem.*, **102**, 6585 (1998).
67 H. Graener, T. Q. Ye, and A. Laubereau, *J. Chem. Phys.*, **90**, 3413 (1989).
68 W. L. Jorgensen, *J. Phys. Chem.*, **90**, 1276 (1986).
69 H. Otaki, S. Itoh, and B. M. Rode, *Bull. Chem. Soc. Jpn.*, **59**, 271 (1986).

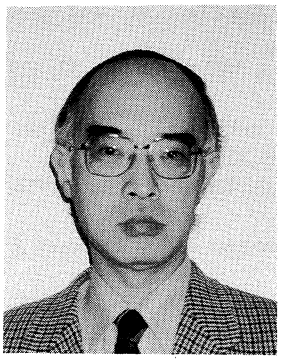

Yoshinori Hirata was born in Chiba, Japan on March 15, 1950. He received B. S. degree in 1972, M. S. degree in 1974 and Ph. D. degree in 1977 from Tokyo Institute of Technology. He spent three years from 1977 as research associate at Wayne State University. In August 1980, he was appointed as research associate in Osaka University. He was appointed as associate professor in the same university in 1995.